Spatiotemporal Brain Imaging: Microscopic&Systems Level (EB00790-02).

Overall goals and objectives

The ability to observe neuronal activity at the macroscopic scale (on the order of millimeters to centimeters) has been advancing rapidly through the development of several non-invasive techniques including PET, fMRI, EEG, and MEG. Although macroscopic neuroimaging can address numerous important questions about human brain function at the systems level, it is often difficult to relate these results to the underlying biophysics and cellular organization of the brain at the microscopic scale. The overall goal of this project is to develop an integrated suite of technologies to bridge this critical gap.

Our main objectives are to improve the spatial and temporal resolution of non-invasive technologies, so that they can resolve more discrete (e.g., column and laminar level) neural units which bridge the systems and cellular levels; and to clarify the mechanisms which relate the biophysics of neuronal activity to "observables" in our imaging measurements. These observables include direct and indirect measures of neuronal activity such as electrophysiology and hemodynamics (blood flow, blood volume, and blood oxygenation). Developing realistic models of brain function requires instruments capable of extreme sensitivity to these observable physiological and biophysical parameters, with high spatial and temporal resolution to measure direct and indirect consequences of brain activity at near-microscopic scales.

Aim 1: Improve fMRI Spatial Resolution in the macaque and rat model

through development of pulse sequence methods, RF array coil technology and gradient coils for ultra-high field imaging (9.4T for rodents and 7T for primates).

Figure 1. Laminar resolution of 7T Structural MRI in primates.

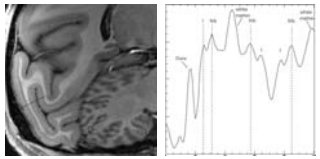

The line of Gennari (layer 4b in V1) is clearly visible in the primary visual cortex of the anesthetized macaque.The left panel shows a sagittal slice, from a 250 um x 250 um x 750 um 3D MPRAGE T1 weighted scan at 7T using a 5 cm receive-only surface coil over primary visual cortex (area V1) in macaque. The right panel shows an intensity profile, taken orthogonal to the cortical surface along the black line overlaid on the image in the top panel. In both the MR image (top) and the corresponding line plot (bottom), he highly-myelinated layer 4B (the stria of Gennari) is prominently differentiable within the center of the gray matter, across three folds of primary visual cortex.

Figure 2. Functional imaging of awake behaving monkey fMRI at 7T.

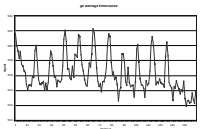

Time course of visual activation produced by a large flickering checkerboard stimulus, recorded without averaging from a single small (1.25 mm isotropic) voxel from primary visual cortex of an awake behaving macaque scanned at 7T. The checkerboard visual stimulus was presented in 4-second blocks separated by blocks of a uniform gray stimulus, while the animal was fixating the center of the stimulus screen.

Figure 3. 3T 4 channel receive-only primate array with dedicated transmit coil.

The arrays consists of 3cm diameter actively detuned coil elements cut on a CAD controlled circuit board milling machine. The array is shown over the monkey head model made from MR data and 3D printing methods to aid in the construction of custom fitted helmets for the individual monkeys used in the fMRI experiments.

Figure 4. Rat fMRI at 9.4T.

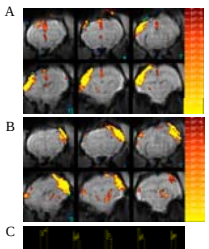

Electrical stimulation of right (A) and left (B) whisker pad. 30 sec stimulation at 3 Hz produces extensive activation of the somatosensory cortex readily observable using our single receive-only surface coils and 0.4mm isotropic resolution epi sequences. The timecourse of activation from active pixels in A is shown in C.

Aim 2: Improve the spatiotemporal resolution of optical imaging

Figure 5. The instrument for simultaneous measurement of blood flow, volume and oxygenation.

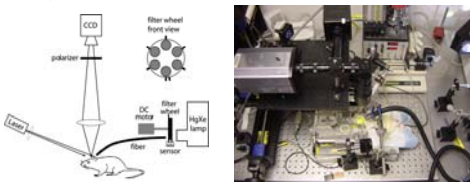

We have developed an imaging instrument that provides simultaneous spectroscopic imaging of intrinsic signals and laser speckle imaging of blood flow. A schematic representation is shown on the left, a close-up image of the experimental setup is on the right.

Figure 6. Multiwavelength imaging of intrinsic signals.

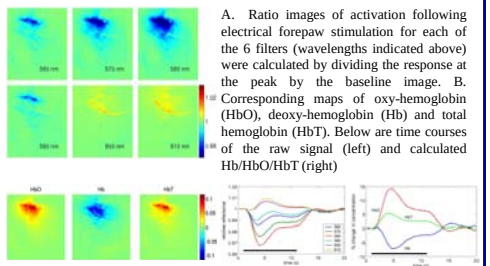

A. Ratio images of activation following electrical forepaw stimulation for each of the 6 filters (wavelengths indicated above) were calculated by dividing the response at the peak by the baseline image. B. Corresponding maps of oxy-hemoglobin (HbO), deoxy-hemoglobin (Hb) and total hemoglobin (HbT). Below are time courses of the raw signal (left) and calculated Hb/HbO/HbT (right)

Figure 7. Laser speckle contrast imaging of cerebral blood flow.

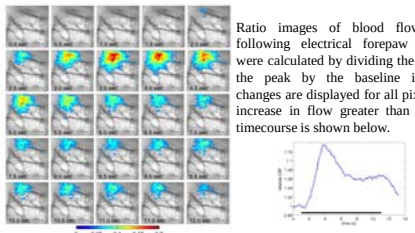

Ratio images of blood flow response following electrical forepaw stimulation were calculated by dividing the response at the peak by the baseline image. The changes are displayed for all pixels with an increase in flow greater than 5%. Signal timecourse is shown below.

Figure 8. Calculation of CMRO2 using simultaneous spectroscopic and speckle contrast imaging.

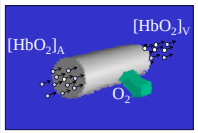

$$CMRO_2 = CBF \cdot (SaO_2 - SvO_2) = CBF \cdot OEF \cdot SaO_2$$

Assume $SaO_2 = 1$

$$\left(1+\frac{\Delta CMRO_2}{CMRO_{2,0}}\right) = \left(1+\frac{\Delta CBF}{CBF_0}\right)\left(1+\gamma_R\frac{\Delta HbR}{HbR_0}\right)\left(1+\gamma_T\frac{\Delta HbT}{HbT_0}\right)$$

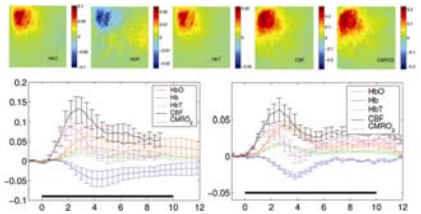

By combining the multi-wavelength imaging with speckle contrast imaging, we calculated the spatio-temporal changes in $CMRO_2$. Ratio images were calculated by dividing the response 1-3 sec after the stimulus onset by the baseline image. The signal is expressed in fractional change. Timecourses for forepaw (left) and whisker (2 sec of upward deflections of a single whisker at 8 Hz, right) stimulation are shown under the images. Stimulus duration is indicated by a bar. Although the spatial localization of $CMRO_2$ is comparable to that of the blood flow, these preliminary results support the hypothesis that temporally $CMRO_2$ activity is more confined to the neuronal response than the hemodynamic measures.

Figure 9. Laminar Optical Tomography (LOT).

LOT uses a system similar to a confocal microscope. The LOT system design allows detection not only of light emerging from the point being illuminated, but also of the scattered light emerging from different relative distances from the illumination point. This light has traveled more deeply in the tissue, and therefore provides images of structures that are much deeper than can be visualized with Confocal microscopy. In addition to the raw images, the data can be used to perform a reconstruction that actually resolves the depth of the features seen..

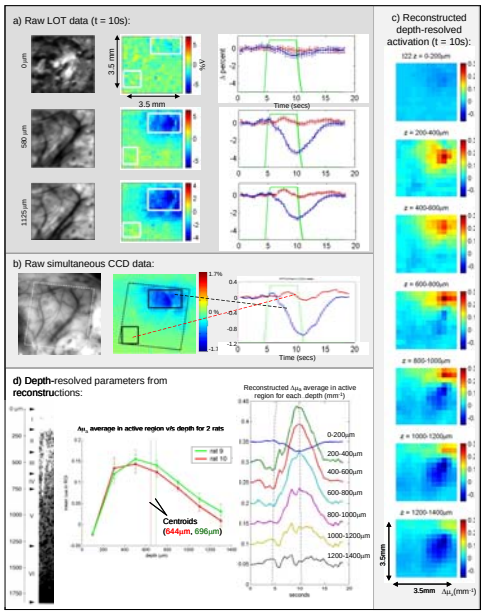

A. Raw LOT data acquired using a 532nm laser, for effective source-detector separations of 0, 0.58mm and 1.125mm. The adjacent images show the % change in detected intensity observed at the time of peak activation following electrical forepaw stimulation. Blue regions indicate a decrease in light corresponding to an increase in hemoglobin. The red and blue temporal traces represent the trends in the signals from the two highlighted regions during the course of the stimulus (shown in green).

B. A CCD image of the same region, taken at the same time as the LOT data using traditional cortical imaging techniques.

C. Tomographically reconstructed images at the peak activation time for different depths. A change in the reconstructed absorption coefficient (μ_a) of 0.3 corresponds to a 30μM hemoglobin change.

D. Data extracted from the whole time-series of reconstructed images, demonstrating that the centroid of the resolved response is around 650-700nm, which corresponds well to cortical layer IV. The LOT results also indicate that the temporal shape of the activation is in fact different at different depths, something that is not revealed using the raw data or the CCD data alone.

Aim 3: Apply the new technologies to image functional activation.

Correlation between hemodynamic imaging signals and the biophysics of neuronal activity.

Figure 10. Spatiotemporal evolution of HbO, Hb and HbT

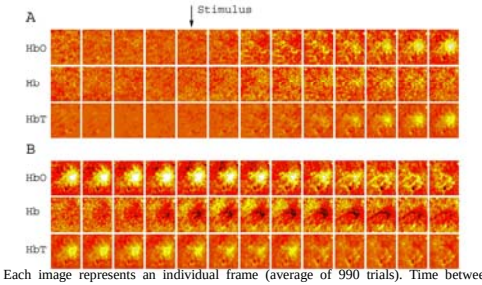

Each image represents an individual frame (average of 990 trials). Time between consecutive images is 200 msec. Panel B is a continuation of the time series shown in panel A. The signal for Hb and HbO is expressed in percent change relative to its own baseline concentration (40 and 60 μM respectively). HbT was calculated as a sum of Hb and HbO.

Figure 11. Signal timecourses of Hb, HbO, and HbT calculated from the data in figure 10.

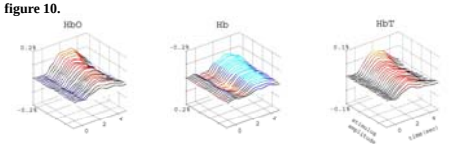

Hemodynamic signals monotonically increase (close to linear) throughout the range of stimulus intensities.

Figure 12. Laminar recordings of neuronal activity using 23 channel depth array.

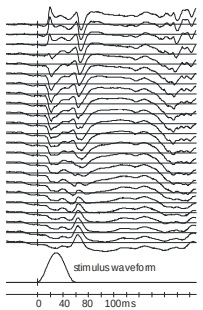

In order to address the laminar pattern of electrophysiological activity, multiple unit activity (MUA) and local field potential (LFP) were measured using a linear array multi-electrode. The figure shows single trial laminar recordings of LFP in response to tactile whisker stimulation. Each trace represents a recording from a single contact as a function of time. The intra-contact distance 100 mm. The most upper contact is on the cortical surface. Stimulus waveform underneath the traces represents a control signal for the piezoelectric stimulating device. Stimulus onset is indicated by a dashed line.

Figure 13. Simultaneous recordings from cortex and thalamus.

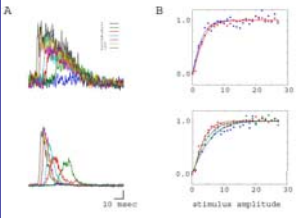

We performed laminar recordings from the active cortical column (principal barrel in Barrel cortex), and the corresponding input location (the corresponding barreloid in the thalamus). A. Thalamic (top) and cortical layer IV (bottom) response to one deflection of a single whisker. Responses using different stimulus amplitudes are superimposed. B. Peak response amplitude as a function of stimulus intensity. Top: cortical layer IVresponse (red) follows that of the thalamus (blue). Bottom: supra- and infragranule layers (green and blue) saturate at a slower rate than layer IV(red).

Figure 14. Hemodynamic response is influenced by neuronal activity in neighboring cortical columns.

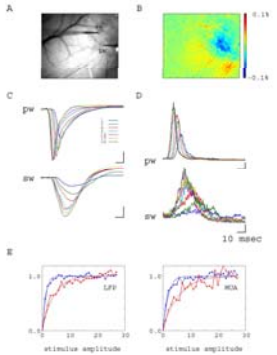

Simultaneous recordings from two neighboring cortical columns (barrels) show that the response in surrounding barrels as a function of stimulus intensity saturates at a slower rate. A. An image of vasculature with two electrodes recording from the principal (pw) and surround (sw) barrels. B. A ration image of response at 580 nm. C-D LFP and MUA. E. Peak amplitude of LFP (left) and MUA (right) in the principal (blue) and surround (red) barrel. Note that the red curved do not reach an asymptote.

Figure 15. Neurovascular transfer function

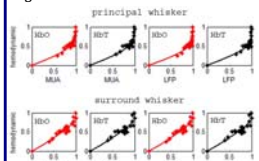

$$y(t) = F(u(t)) \otimes h(t)?$$

y(t) and u(t) are the measured hemodynamic and electrophysiological signals, respectively. F represents a stationary nonlinearity, and h(t) the hemodynamic impulse response function.

- An increase in the hemodynamic response beyond saturation of local pre- and postsynaptic activity indicates that vascular responses do not have a single column resolution
- Point measurement of neuronal response does not reflect point hemodynamic activity. However, the relationship between local hemodynamic activity and neuronal activity in the same area is supralinear
- The neuronal activity cannot be inferred from a point hemodynamic measurement. Surround hemodynamic "inhibition" does not correspond to a decrease in neuronal activity